



## **A NOVEL CARCINOEMBRYONIC ANTIGEN T CELL BISPECIFIC ANTIBODY (CEA TCB) FOR THE TREATMENT OF SOLID TUMORS**

Marina Bacac<sup>1</sup>, Tanja Fauti<sup>1</sup>, Johannes Sam<sup>1</sup>, Sara Colombetti<sup>1</sup>, Tina Weinzierl<sup>1</sup>, Djamila Ouaret<sup>2</sup>, Walter Bodmer<sup>2</sup>, Steffi Lehmann<sup>3</sup>, Thomas Hofer<sup>4</sup>, Ralf J. Hosse<sup>4</sup>, Ekkehard Moessner<sup>4</sup>, Oliver Ast<sup>4</sup>, Peter Bruenker<sup>4</sup>, Sandra Grau-Richards<sup>4</sup>, Teilo Schaller<sup>1</sup>, Annette Seidl<sup>5</sup>, Christian Gerdes<sup>1</sup>, Mario Perro<sup>1</sup>, Valeria Nicolini<sup>1</sup>, Nathalie Steinhoff<sup>1</sup>, Sherri Dudal<sup>6</sup>, Sebastian Neumann<sup>7</sup>, Thomas von Hirschheydt<sup>8</sup>, Christiane Jaeger<sup>4</sup>, Jose Saro<sup>9</sup>, Vaios Karanikas<sup>9</sup>, Christian Klein<sup>1\*</sup>, Pablo Umaña<sup>1</sup>

Roche Pharmaceutical Research & Early Development, <sup>1</sup>Oncology Discovery, <sup>4</sup>Large Molecule Research, <sup>9</sup>Translational Medicine, Roche Innovation Center Zurich; <sup>6</sup>Pharmaceutical Sciences, Roche Innovation Center Basel; <sup>8</sup>Large Molecule Research, Roche Innovation Center Penzberg; <sup>2</sup>Cancer & Immunogenetics Laboratory, Weatherall Institute of Molecular Medicine, John Radcliffe Hospital, Oxford OX3 9DS, UK; <sup>3</sup>Animal Imaging Center, Institute for Biomedical Engineering, ETH and University of Zurich, Vladimir-Prelog Weg 4, Switzerland; <sup>5</sup>Roche Diagnostics GmbH, Penzberg, Germany; <sup>7</sup>Roche Diagnostics GmbH F. Hoffmann-La Roche AG, Division Pharma, PTDM, Basel, Switzerland

\* both authors contributed equally

**Running title:** CEA TCB antibody targeting solid tumors

**Keywords:** Cancer Immunotherapy, Bispecific antibody, CEA, T cell, cytotoxicity

 **Corresponding authors:**

Marina Bacac [marina.bacac@roche.com](mailto:marina.bacac@roche.com) and Pablo Umaña [Pablo.umana@roche.com](mailto:Pablo.umana@roche.com)

Roche Pharma Research & Early Development, Roche Innovation Center Zurich

Roche Glycart AG, Wagistrasse 18, 8952 Schlieren, Switzerland

Phone: +41 44 755 61 41/61 34

Fax: +41 44 755 61 65

**Conflicts of interests.** All authors (except Walter Bodmer and Djamila Ouaret) are (or were at the time when the study was conducted) Roche employees.

**Word count:** 5052 (excluding Abstract, Statement of Translational Relevance, Acknowledgements, Figure legends)

**Total number of figures and tables:** 5 figures, 3 supplemental figures, 2 supplemental tables, 2 videos

## **Statement of translational relevance**

The study provides novel mechanistic insights into the design and activity of CEA TCB, an IgG-based T cell bispecific antibody (TCB) currently in Phase 1 clinical trials (NCT02324257). Its novel design confers long circulatory half-life along with selective tumor targeting, intra-tumor T-cell activation and killing without peripheral blood immune cell activation. In addition to the novel molecular features of the TCB format, the manuscript provides insights into interesting aspects related to the biological activity of CEA TCB, including a threshold of CEA receptors required for activity, selectivity for high CEA-expressing tumor cells, efficacy in non-inflamed and poorly T cell-infiltrated tumors and the ability to increase T cell infiltration in tumors thus converting the non-inflamed, PD-L1 negative tumors into highly-inflamed and PD-L1 positive tumors resulting in the generation of a more inflamed tumor microenvironment.

## Abstract

**Purpose:** CEA TCB is a novel IgG-based T Cell Bispecific antibody for the treatment of CEA-expressing solid tumors currently in Phase 1 clinical trials (NCT02324257). Its format incorporates bivalent binding to CEA, a head-to-tail fusion of CEA and CD3e binding Fab domains and an engineered Fc region with completely abolished binding to FcγRs and C1q. The study provides novel mechanistic insights into the activity and mode of action of CEA TCB.

**Experimental design:** CEA TCB activity was characterized on 110 cell lines in vitro and in xenograft tumor models in vivo using NOG mice engrafted with human PBMCs.

**Results:** Simultaneous binding of CEA TCB to tumor and T cells leads to formation of immunological synapses, T cell activation, secretion of cytotoxic granules and tumor cell lysis. CEA TCB activity strongly correlates with CEA expression, with higher potency observed in highly CEA-expressing tumor cells and a threshold of approximately 10,000 CEA binding sites/cell, which allows distinguishing between high- and low-CEA expressing tumor and primary epithelial cells, respectively. Genetic factors do not affect CEA TCB activity confirming that CEA expression level is the strongest predictor of CEA TCB activity. In vivo, CEA TCB induces regression of CEA-expressing xenograft tumors with variable amounts of immune cell infiltrate, leads to increased frequency of activated T cells and converts PD-L1 negative into PD-L1 positive tumors.

**Conclusion:** CEA TCB is a novel generation TCB displaying potent anti-tumor activity; it is efficacious in poorly-infiltrated tumors where it increases T cell infiltration and generates a highly-inflamed tumor microenvironment.

## Introduction

Redirecting the activity of T cells by bispecific antibodies against tumor cells, independently of their TCR specificity, is a potent approach to treat cancer (reviewed in (1-3)). The concept is based on recognition of a cell surface tumor antigen and simultaneous binding to the CD3 epsilon chain (CD3e) within the T cell receptor (TCR) complex on T cells. This triggers T cell activation, including release of cytotoxic molecules, cytokines and chemokines and induction of T cell proliferation (1, 2).

The first T cell bispecific antibody was described 30 years ago (4), but it was only recently that the first TCB for systemic administration to cancer patients, blinatumomab, an anti-CD19  $\times$  anti-CD3e TCB, was approved by the U.S. Food and Drug Administration (FDA) for the treatment of relapsed/refractory B cell acute lymphocytic leukemia (B-ALL) (5). A major limitation of the earlier TCB molecules was that they induced strong cytokine release and resulted in severe infusion related reactions, which precluded their systemic administration. Indeed such an earlier TCB, catumaxomab, targeting EpCAM, could only be applied for local, peritoneal administration for the treatment of malignant ascites (6). Besides being highly immunogenic in humans (as rat/mouse hybrid monoclonal antibody), catumaxomab carries an active Fc domain capable of crosslinking Fc $\gamma$ Rs on innate immune cells and CD3e on T cells, which leads to strong cytokine release upon systemic administration, independently of tumor target cell binding (7). This limitation was overcome in blinatumomab by removing the Fc domain and linking the anti-CD19 and anti-CD3e domains via a short, flexible Gly-Ser linker (3). However, by removing the Fc region, protection from catabolism via FcRn recycling was eliminated and this, together with the small molecular size of blinatumomab, leads to fast drug clearance. Indeed, blinatumomab has to be administered via continuous infusion for several weeks (5), an approach which would significantly limit the application of

TCBs to the majority of cancer patients. Thus new TCB molecular formats with comparable or higher efficacy than blinatumomab, but with significantly longer circulatory half-life allowing for systemic administration every few weeks and at the same time avoiding peripheral immune cell activation and cytokine release in the absence of target engagement, are desired.

Another obstacle to the broad utilization of TCBs is the availability of suitable, tumor-specific targets. Most solid tumor targets are overexpressed on tumor cells but expressed at lower, yet significant levels on non-malignant primary cells in critical tissues. In nature, T cells can distinguish between high and low antigen expressing cells by means of relatively low affinity TCRs that can still achieve high avidity binding to target cells expressing sufficiently high levels of target antigen. Molecular TCB formats that could accomplish the same, and thus maximize the window between killing of high- and low-target expressing cells, would be highly desirable.

The current manuscript highlights the novel molecular features of CEA TCB (RG7802; RO6958688; Fig.1A), which is the only IgG-based CEA T cell bispecific antibody that entered clinical trials to date ((8), NCT02324257) and is differentiated from previously-described scFv or diabody-based T cell bispecific antibodies targeting CEA. CEA, also called carcinoembryonic antigen related cell adhesion molecule 5 (CEACAM5) or CD66e, is a 180-200 kDa protein that belongs to the CEACAM superfamily and is anchored to the cell surface via glycosylphosphatidylinositol (GPI). CEA expression in various tumor entities is generally very high, especially in colorectal carcinoma (CRC), pancreatic adenocarcinoma (PanCa), gastric cancer (GC), non-small cell lung cancer adenocarcinoma (NSCLC), breast cancer (BC), head and neck carcinoma (HNSCC), uterine and bladder cancers amongst others (9). Low expression is found in small cell lung cancer and glioblastoma (10-15). CEA is expressed at low levels on the apical surface of glandular epithelia in the gastrointestinal (GI)

tract, but its polarized expression pattern limits accessibility to therapeutic antibodies administered systemically (10, 11, 16, 17). In addition to the novel molecular features of the TCB format, the manuscript provides insights into interesting aspects related to the biological activity of CEA TCB, including a threshold of CEA receptors required for activity, selectivity for high CEA-expressing tumor cells, efficacy in non-inflamed and poorly T cell-infiltrated tumors and the ability to increase T cell infiltration in tumors thus generating a more inflamed tumor microenvironment.

## Materials and Methods

**Cells, CEA expression level and antibody binding.** The list of all cell lines used in the study, their source and authentication is provided in Table S1. The cell line panel (C10, C106, C10A, C10S, C125PM, C2BBel, C32, C70, C75, C80, C99, CACO2, CAR1, CC20, CCK81, CCO7, CL11, CL14, CL40, COCM1, COLO201, COLO205, COLO206, COLO320DM, COLO320HSR, COLO678, CW2, CX1, DLD1, GP2d, GP5d, HCA46, HCA7, HCC2998, HCC56, HCT116, HCT15, HDC111, HDC114, HDC135, HDC142, HDC143, HDC54, HDC57, HDC73, HDC8, HDC82, HDC9, HRA19, HT29, HT55, ISRECO1, JHCOLOYI, JHSK-rec, KM20L2, LIM1215, LIM1863, LIM2405, LOVO, LS1034, LS123, LS174T, LS180, LS411, LS513, NCIH508, NCIH548, NCIH716, NCIH747, OUMS23, OXCO1, OXCO2, OXCO3, PCJW, PMFKO14, RCM1, RKO, RW2982, RW7213, SKCO1, SNU1181, SNU1235, SNU1411, SNU1544, SNU1684, SNU1746, SNU254, SNU479, SNU70, SNU977, SNUC1, SNUC2B, SW1116, SW1222, SW1417, SW1463, SW403, SW48, SW480, SW620, SW837, SW948, T84, TT1TKB, VACO10MS, VACO429, VACO4A, VACO4S, VACO5 and WIDR) has been accumulated over a period of more than 25 years and, in many cases, cell lines were obtained from their originators before they became available from commercial cell banks. C10, C106, C125PM, C32, C70, C75, C80 and C99 cell lines have been established in the Cancer Immunogenetics Laboratory (Walter Bodmer) and have been deposited at the European Collection of Cell Cultures (ECACC). Authentication of the cell line panel mentioned above was performed in the Bodmer Laboratory using a carefully-designed and fully-validated custom panel of 34 un-linked single nucleotide polymorphisms (SNPs) using the Sequenom MassARRAY iPLEX technology. Authentication was carried out at least once every year and, in general, at the time of preparation of the frozen cell stocks used for the TCB response assays. The most recent genotyping was performed on 58 of the cell line panel in August 2014 (Table S1). 19 cell lines were also screened using the



HumanOmniExpress-24 BeadChip arrays (>700k SNPs) in April 2014 (Table S1). The cell line panel mentioned above has also been characterized for RER status and for driver mutations in following genes: *APC*, *TP53*, *CTNNB1*, *KRAS*, *BRAF*, *PIK3CA* and *FBXW7*. All cell lines were obtained more than 6 months before the start of the experiments described in this paper and all were tested regularly for absence of mycoplasma using the MycoAlert™ Mycoplasma Detection Kit (Lonza).

### **Assessment of tumor cell lysis, cytokine secretion and T cell activation mediated by**

**CEA TCB.** Human PBMCs were purified from fresh blood of healthy donors by conventional Histopaque gradient (Sigma-Aldrich). Adherent target cells were trypsinized (0.05 % trypsin/EDTA; Gibco) and 30 000 cells/well were seeded in flat-bottom-96-well-plates (TPP). CEA TCB or control molecules and human PBMC effector cells were added (E:T ratio of 10:1). All samples were performed in triplicates. Target cell killing was assessed after 24 h and 48 h of incubation at 37°C, 5% CO<sub>2</sub> by quantification of LDH released into cell supernatants by dead cells (LDH detection kit, Roche Applied Science). Maximal lysis of the target cells (= 100%) was achieved by incubation of target cells with 1% Triton X-100. Minimal lysis (= 0%) refers to target cells incubated with effector cells without TCB. Percentage of specific cell lysis was calculated as [sample release - spontaneous release]/[maximum release - spontaneous release] x 100. Cytokines secretion was assessed 48 h post incubation of target cells with CEA TCB and PBMCs (as above). Cytokines (Granzyme B, TNF, IFN- $\gamma$ , IL-2, IL-4 and IL-10) were measured by FACS analysis using the BD CBA Human Soluble Protein Flex Set with 50  $\mu$ l of undiluted supernatant, according to manufacturer's instructions. Data were acquired using FACS CantoII and EC50 values calculated using GraphPadPrism5. T cell activation was evaluated by FACS analysis 48 h post incubation of target cells with CEA TCB and PBMCs (as above). PBMCs were transferred into new 96-round-bottom well plates, washed once and stained for 30 min at 4°C

with antibody mix (CD4, CD8, CD69, CD25, BD or BioLegend) according to the suppliers' indications. After two washing steps, samples were analyzed by flow cytometry.

**Mice.** NOG female mice (NOD/Shi-*scid*/IL-2R $\gamma^{\text{null}}$ , purchased from Taconic), aged 6-8 weeks at experiment initiation, were maintained under specific-pathogen-free condition with daily cycles of 12 h light /12 h darkness according to committed guidelines (GV-Solas; Felasa; TierschG). Experimental study protocol was reviewed and approved by local government authorities (P2011128). After arrival, animals were maintained for one week for observation and for adaptation to the new environment. Continuous health monitoring was carried out on a daily basis.

**Tumor/PBMC co-grafting setting.** LS174T-fluc2 cells ( $1 \times 10^6$  cells) were admixed with freshly-isolated human PBMC at the indicated effector:target (E:T) ratios of 5:1 or 1:1. Tumor cell/PBMC mixture was co-grafted (injected) s.c. in NOG mice in a total volume of 100  $\mu$ l in RPMI medium. Therapy administration i.v. (200  $\mu$ L) was performed either 1 or 7 days after co-grafting at the indicated doses and schedules.

**Tumor model with IP transfer of PBMC.** NOG mice were injected s.c. with LS174T-fluc2 cells ( $1 \times 10^6$  cells) and tumor volume measured twice/week by caliper and bioluminescence imaging (BLI). Mice were injected with human PBMC i.p. ( $10 \times 10^6$  cells), 7 days after tumor cell injection. Therapy administration started after 3 days of PBMS transfer (i.e. 10 days after tumor cell injection, all groups), followed by i.v. injection of 200  $\mu$ L of CEA TCB, untargeted TCB or phosphate buffer saline (PBS, vehicle), all twice/week.

**Monitoring of tumor growth.** Animals were controlled daily for clinical symptoms and detection of adverse events. Tumor volume was measured by digital caliper every second day or by bioluminescence imaging (BLI) that allows non-invasive and longitudinal monitoring of tumor growth. BLI acquisitions (photons/sec) were performed twice a week by intra-

peritoneal injection of 200 $\mu$ L luciferin substrate (15mg/kg). The signal was followed over time and detected using the IVIS® Spectrum (PerkinElmer). Data were analyzed with the Living Image software.

**Histological Analysis.** Tumor tissues from termination animals were fixed in 4% PFA (Paraformaldehyde) overnight and embedded in paraffin. Briefly, 4  $\mu$ m Sections were cut using a Microtome (Leica) and mounted on glass slides. Samples were de-paraffinized and heat antigen retrieval was performed prior to immune-staining for human CEA (Roche), human CD3 (Abcam), human CD45 (Ventana), human CD8 (Abcam) and human PD-L1 (Ventana). The sections were counterstained with hematoxylin (Sigma Aldrich) and slides scanned using Olympus VS120-L100.

## Results

**Structural characteristics and binding properties of CEA TCB.** CEA TCB is an IgG1-based bispecific heterodimeric antibody that binds with one arm to CD3epsilon chain (CD3e) expressed on T cells and with two arms to CEA expressed on tumor cells (Fig. 1A). The correct association of light chains of the antibody is enabled by introducing a CH1-CL crossover into the internal CD3 binding Fab (18), whereas correct heavy chain association is facilitated via the knob-into-hole technology (19, 20). CEA TCB binds to human CEA-expressing tumor cells bivalently with avidity of 10 nM (Fig.1B), and targets a membrane-proximal domain of human CEA (21, 22). The CEA binder used in CEA TCB (named CH1A1A) is a humanized, affinity matured and stability-engineered version derived from the PR1A3 antibody (23, 24). As the membrane-proximal domain of CEA is not conserved among species, CEA TCB binds specifically to human CEA and does not cross-react with Cynomolgus monkey CEA (Fig.S1 A). In addition, CEA is not expressed in rodents so CEA

TCB also lacks cross-reactivity with mice and rats. Due to targeting of a membrane-proximal domain of human CEA, CEA TCB displays preferential binding to membrane-anchored CEA rather than to shed CEA (sCEA), and the binding to CEA-expressing cells is not affected up to concentration of 5 ug/mL of sCEA (Fig.S1 B). In addition, the binding of the CEA antibody included in CEA TCB does not affect tumor cell proliferation (not shown), or result in internalization (Fig.S1 C). CEA TCB binds to CD3 epsilon chain (CD3e) of the TCR-complex with its monovalent CD3 Fab (21). The humanized anti-CD3e antibody included in CEA TCB cross-reacts with human and Cynomolgus monkey CD3e (Fig.1 C, Fig.S1 D and Fig.S1 E), but not with mouse CD3e since the targeting epitope is not conserved in rodents (Fig.S1 F). The binding to CD3e is monovalent (to prevent T cell activation in the absence of simultaneous binding to CEA-expressing tumor cells), and has low affinity for both human and Cynomolgus monkey CD3e (100 nM in Biacore measurements) to reduce the peripheral binding to T cells and facilitate the preferential binding to CEA-expressing tumor cells. CEA TCB is a human IgG1 with the heterodimeric Fc region conferring an extended half-life (Fig.S2 A-C) as compared to non-Fc-containing T cell bispecific antibodies (5, 25-27). The Fc part of CEA TCB bears a novel, proprietary modification (Pro329Gly combined with Leu234Ala/Leu235Ala, here referred as P329G LALA mutation, Fig.1 A), which abrogates its binding to complement component (C1q) and to Fc gamma receptors (FcγR) and prevents FcγR-mediated co-activation of innate immune effector cells in vitro, including natural killer (NK) cells, monocytes/macrophages, and neutrophils, without changes in functional binding to FcRn (neonatal Fc receptor), (manuscript in preparation,(28)). CEA TCB is therefore devoid of complement-dependent cellular cytotoxicity (CDC) and antibody-dependent cellular cytotoxicity (ADCC) activity, (Fig.S1 G and H), with T cells being the only immune effector cells engaged by CEA TCB.

**Mode of action of CEA TCB.** Upon simultaneous binding to CEA-expressing tumor cells and CD3-expressing T cells, CEA TCB rapidly crosslinks T cells to tumor cells, leading to the activation of the CD3 downstream signaling pathway (Fig.2 A), and formation of the immunological synapses, as observed by imaging of talin clustering, MTOC re-localization and perforin re-distribution at the interface between tumor cells and T cells (Fig.2 B-C). T cell activation ( $CD8 > CD4$ ) is further reflected by the expression of activation markers detected as early as 8.5 h post addition of CEA TCB to co-cultures of CEA-expressing tumor cells and human PBMCs (Fig.2 D - E), finally leading to time- and dose-dependent lysis of tumor cells (Fig.2 F). As further hallmark of T cell activation upon tumor lysis, a number of cytokines were detected in culture supernatants, including interferon gamma (IFN $\gamma$ ), tumor necrosis factor (TNF), interleukin (IL)-2, IL-6, IL-10 as well as cytotoxic granule granzyme B (Fig.2 G). Following CEA TCB-mediated tumor lysis, both CD8 and CD4 T cell subsets undergo dose-dependent proliferation (Fig.2 H, CD8 T cell subsets slightly more than CD4 T cells), and maintain an activated phenotype as shown by expression of the late activation marker CD25 (Fig.2 I, CD8 T cell subsets slightly more than CD4 T cells). Treatment of tumor/PBMC co-cultures with untargeted TCB (a control TCB that binds to T cells but does not bind to any tumor antigen and thus cannot cross-link T cells), does not lead to any activities described above (Fig.2 B, C, H; Fig.S2 D-G), further confirming that CEA TCB activity is CEA-specific and strictly dependent on its expression.

**Correlation between CEA expression and CEA TCB activity.** Initial analysis of CEA TCB-mediated tumor cell lysis performed on a limited number of CEA-expressing tumor cells and primary epithelial cells pointed out a possible correlation between CEA TCB activity and CEA expression (Fig. 3 A). To further corroborate the initial findings, CEA TCB activity was assessed on a panel of 110 colorectal cancer cell lines (CRC) expressing various levels of surface CEA (Table S1), therefore representing a larger and better diversity in the

pattern of CEA expression. In general, there were two major groups of target cells displaying < 10% (non-responders, red squares) and > 10 % (responders, blue squares) of tumor lysis (Fig. 3 B). When looking at CEA expression, we noticed that the non-responder group had predominantly (with only few exceptions) < 10 000 CEA binding sites, whereas the cell lines belonging to the responder group were characterized by > 10 000 CEA binding sites (Fig. 3 B and C). A comparison of the CEA expression level between the two groups showed statistically highly significant difference in CEA expression (Fig. 3 C, \*\*\*\*p<0.0001), suggesting a strong and robust correlation between CEA expression level on target cells and CEA TCB activity. Interestingly, the tests performed to look for associations between the major genetic changes found in colorectal carcinomas and the response to CEA TCB therapy, including correlations with the replication error (RER) status and mutations in *APC*, *TP53*, *CTNNB1*, *KRAS*, *BRAF*, *PIK3CA* and *FBXW7*, did not result in any significant correlation (Table S2), further suggesting that, based on in vitro data, CEA expression level appears to be the strongest predictor of CEA TCB activity.

**In vivo activity of CEA TCB.** The anti-tumor activity of CEA TCB was initially assessed using a human colon carcinoma xenograft model (LS174T) stably expressing firefly luciferase (LS174T-fluc2), co-grafted with human PBMCs at E:T ratios of 5:1 and 1:1 (Fig. 4 A-D). Mixed cells were injected s.c. in immunodeficient NOG mice. Treatment schedules of CEA TCB were selected based on single-dose PK profile (SDPK) of i.v. bolus injection of CEA TCB in NOG mice (Fig.S2 A-C). CEA TCB, untargeted TCB (both given at 2.5 mg/kg) or vehicle (PBS) were administered twice/week starting either one day or seven days post tumor/PBMC co-grafting (red arrow). CEA TCB mediated strong tumor growth inhibition when administered either one day or seven days after tumor/PBMC co-grafting at both E:T ratios (E:T 5:1, Fig. 4 A, B and E:T 1:1 Fig. 4 C, D). On the contrary, in control groups (treated with PBS (vehicle) or untargeted TCB) tumors continued growing (Fig. 4 A-D).

CEA TCB activity was further monitored by live imaging using intravital two-photon (2P) microscopy (Fig. 4 E). To this end, LS174T-RFP cells (RFP=red fluorescence protein, red) were mixed with human PBMCs at an E:T ratio of 5:1 (T cells were labeled with CFSE, green) and co-grafted into a dorsal skinfold chamber surgically mounted on mice 24 hours before cell injection. Microscopic imaging of tumors performed 4 days post tumor cell/PBMC co-grafting (baseline analysis), revealed a significantly decreased E:T ratio most likely due to fast proliferation of tumor cells and dissemination of T-cells from the primary tumor via tumor associated blood/lymphatic vessels. These results indicate that, despite an initial E:T of 5:1 at the time of co-grafting, tumors rapidly change their composition and evolve into masses predominantly containing tumor cells (Fig. 4 E, baseline). After baseline image acquisition, mice received a single dose of CEA TCB or untargeted TCB (both at 2.5 mg/kg) and imaging was repeated 1 day (Fig. 4 E and Video 1 and Video 2) and 6 days (Fig. 4 E) after treatment. Microscopic images acquired 1 day after treatment revealed a significant increase in the number of fragmented tumor cells (indicative of apoptosis) along with a substantial increase of intra-tumor T cells upon CEA TCB administration but not upon the treatment with the untargeted TCB (Fig. 4 E and Video 1 and Video 2). Furthermore, there was a strong presence of tumor-associated T cells in animals treated with CEA TCB but not in the ones treated with untargeted TCB (Fig. 4 E and Video 1 and Video 2). Subsequent imaging, performed 7 days after TCB administration in separate animals further demonstrated a significant difference in the number of tumor cells between controls and CEA TCB-treated tumors, with a decreased number of tumor cells present in mice treated with CEA TCB compared to those treated with untargeted TCB (Fig. 4 E). Together, the tumor growth inhibition and two-photon imaging data generated in preclinical mouse tumor models revealed that CEA TCB displays potent anti-tumor activity independently of the baseline immune cell infiltration.

Subsequently, the *in vivo* efficacy of CEA TCB was further confirmed in a xenograft model in which human effector cells were not directly co-grafted with tumor cells, but have to (eventually) traffic from the periphery and be recruited at tumor sites provided that the CEA TCB treatment is efficacious. For that purpose, tumor cells were initially injected s.c. into NOG mice followed by i.p. transfer of human PBMC ( $10 \times 10^6$  cells) once tumors reached a palpable mass ( $100 - 150 \text{ mm}^3$ ). Therapeutic treatment started 3 days after PBMC transfer with CEA TCB and untargeted TCB administered at 2.5 mg/kg, twice/week. Vehicle (PBS) administration was added as an additional control group. Despite the low initial number of tumor-infiltrating lymphocytes, CEA TCB treatment led to a statistically significant tumor regression as compared to controls (Fig. 5 A-B,  $*p < 0.05$ ), along with a strong increase of T cell infiltration into tumors as detected by the flow cytometry analysis (from  $0.1 - 1.9 \pm 0.67$  % in controls to  $25.2 \pm 7.4$  % in CEA TCB treatment groups, Fig. 5 C, tumor panels). Furthermore, intra-tumor T cells displayed an activated phenotype upon CEA TCB treatment with up-regulation of CD25 activation marker and PD-1 exhaustion marker (hallmarks of TCR engagement), (Fig. 5 D, tumor panels). This was in contrast to mice treated with vehicle (PBS) or untargeted TCB, where tumor-infiltrated T cells showed no upregulation of those markers (Fig. 5 D, tumor panels, compare the red line of CD25 and PD-1 expression upon CEA TCB treatment to green and blue line of controls). Importantly, flow-cytometry analysis of blood did not reveal any increase in T cell frequency or activation status, further confirming that CEA TCB activity is restricted to CEA-expressing tumor areas (Fig. 5 C and D, blood panels). Histological staining of tumors collected at study termination confirmed the low infiltration of intra-tumor T cells in controls and their increased frequency upon CEA TCB treatment (both CD4 and CD8 T cell subsets) (Fig. 5 E) along with their massive re-localization from the periphery (predominantly observed in the vehicle and untargeted TCB controls) into the tumor bed (Fig. 5 E, zoomed insets 1 and 2 displaying CD3 localization).



The staining of the same tumors with anti-PD-L1 antibody demonstrated an induction of intra-tumor PD-L1 expression upon CEA TCB treatment as compared to control (Fig. 5 F).

Together, data from in vivo PBMC transfer experiments indicate that CEA TCB is able to induce regression of poorly-infiltrated and non-inflamed solid tumors and to convert them into highly-inflamed, PD-L1-expressing tumors with increased frequency of intra-tumor T cells displaying an activated phenotype. More importantly, CEA TCB treatment induces re-localization of T cells from tumor periphery into tumor bed.

## **Discussion**

CEA TCB is a novel IgG-based T Cell Bispecific (TCB) antibody for targeting of CEA-expressing solid tumors. CEA TCB is the only IgG-based CEA T cell bispecific antibody that entered clinical trials to date (NCT02324257) and is differentiated from previously-described scFv or diabody-based T cell bispecific antibodies targeting CEA, including MEDI-565/AMG 211 (29, 30) or others (31, 32). CEA TCB molecule bears several technological features including i) bivalent binding to CEA, ii) head-to-tail fusion via a flexible linker of the CEA and CD3e binding Fab domains, iii) an engineered, heterodimeric Fc region with completely abolished binding to FcγRs and complement component C1q, and iv) a robust production process based on standard manufacturing steps enabled by the combination of CrossMAb and knob-into-hole technologies (18, 33). The bivalency for the tumor antigen confers high binding avidity to the tumor and translates into better tumor targeting and retention as compared to antibodies having monovalent binding to CEA (Fig. S3 A-E); it also allows a better differentiation between high and low CEA-expressing tumor cells (Fig. 3). The head-to-tail fusion geometry ensures potency similar to the first-generation bispecific T cell engagers (BiTEs), and the fully silent Fc (P329G LALA mutation) extends the molecule's half-life and reduces the risk of FcγR-mediated infusion reactions as it abrogates

interactions with Fc $\gamma$ R-expressing cells including neutrophils, monocyte/macrophages and NKs (28).

Simultaneous binding of CEA TCB to CEA-expressing tumor cells and CD3e-expressing T cells leads to T cell crosslinking to tumors, T cell activation and secretion of cytotoxic granules, ultimately resulting in tumor cell lysis. CEA TCB-mediated tumor lysis is CEA-specific and does not occur in the absence of CEA expression or in the absence of simultaneous binding (cross-linking) of T cells to CEA-expressing tumor cells. Moreover, CEA TCB activity strongly correlates with CEA expression, with higher potency observed in highly CEA-expressing tumor cells with a threshold of approximately 10,000 CEA binding sites/cell required for efficient tumor cell killing. In line with this, CEA TCB was unable to induce T cell-mediated killing of primary epithelial cells expressing < 2,000 CEA binding sites/cell in vitro (Table S1 and Fig. 3 A). Interestingly, the correlation performed to assess any association between the major genetic changes described in colorectal cancer and the response to CEA TCB therapy, including correlations with the replication error (RER) status, mutations in APC, TP53, CTNNB1, KRAS, BRAF, PIK3CA and FBXW7, did not result in any significant correlation further suggesting that, based on in vitro data, CEA expression level appears to be the strongest predictor of CEA TCB activity.

The high avidity binding to CEA conferred by the antibody's design, together with the bivalent binding mode to tumor antigen, translates into a selective killing of high CEA-expressing tumor cells and sparing of the normal epithelial cells. This finding, along with the knowledge that primary epithelial cells express low levels of CEA inaccessible to therapeutic antibodies (due to its polarized expression pattern facing glandular lumen (11, 34, 35), provides confidence into a wide safety window of CEA TCB to select between primary and malignant cells. This is particularly relevant considering that there were no relevant pre-

clinical animal models for the non-clinical toxicology assessment of CEA TCB and that the Entry into Human (EiH) starting dose was calculated using the MABEL approach (manuscript in preparation) and in light of the outcome of a recent clinical trial with CEA TCR T cells (autologous T lymphocytes engineered to express a murine T cell receptor (TCR) against human CEA) in patients with metastatic colorectal cancer refractory to standard treatments (36). Despite all patients showing responses, there was dose-limiting toxicity due to severe transient inflammatory colitis. In addition to the CEA threshold and expression pattern described above, a major difference between this TCR T cell-based study and our approach consists in the cross-linking of high numbers of in vitro expanded/activated T cells that target CEA through a natural T cell receptor (CEA TCR), contrary to our approach that aims at redirecting the activity of the patient's own T cells, most of which are expected to be exhausted by the tumor microenvironment (37, 38). In addition, engineered T cells require a significantly lower target threshold for killing of tumor cells (10-100 times lower) than T cells engaged by therapeutic antibodies (39), and recognize CEA peptides presented by MHC molecules that are localized uniformly along the whole membrane of normal epithelial cells and are not polarized on apical membrane subdomains as is the case for full-length CEA expressed on normal cells. CEA peptides presented by MHC complexes thus easily expose normal epithelial cells to the activity of highly active CEA-specific T cells, as is the case for TCR T cells. Similar differences in the ability to induce toxicities of T cells targeting CEA but expressing TCRs or CARs (Chimeric Antigen Receptor) were recently described by Magee MS (40). This and other studies also highlighted that the CEA expression level in the target organ is a key determinant in the development of toxicity and concluded that, similarly to CEA TCB antibody, CAR T cells can discriminate between cells with varying levels of antigen-expression in vivo, providing a potential avenue to target antigens that are highly expressed by tumor cells but have lower expression in normal tissues (40, 41).

In addition to tumor cell killing, our study unravels novel elements related to the TCB mode of action and provides mechanistic insights into T cell/CD3 activation, formation of immunological synapses, T cell activation and proliferation (expansion) upon TCB trigger. Our data show that immunological synapses form as early as 20 minutes following CEA TCB addition to co-cultures of tumor cells and T cells, and similarly to what is described for endogenous recognition via TCR/MHC-peptide complexes (42, 43), results in rapid clustering of talin at the interface between tumor cells and T cells, followed by MTOC re-localization and perforin polarization towards immunological synapse. We further provide evidence of T cell activation following tumor cell killing upon CEA TCB treatment as detected by upregulation of activation markers (CD69 and CD25), cytokine secretion (IFN $\gamma$ , TNF, IL-2, IL-6, IL-10), cytotoxic granules secretion (granzyme B), as well as T cell proliferation (expansion) of both CD8 and CD4 T cell subsets. T cell expansion has not only been detected in vitro but also in animal studies in vivo.

In vivo CEA TCB induced dose- and time-dependent regression of CEA-expressing xenograft tumors with variable amounts of immune cell infiltrate. More interestingly, CEA TCB was efficacious even in settings in which T cells were not directly present in tumor nodules at the beginning of therapy. In such cases, tumor regression was accompanied by increased number of tumor-infiltrating leukocytes (TILs), reflecting T cell recruitment and/or intra-tumor T cell expansion/proliferation, along with a remarkable T cell re-localization from the tumor periphery into the tumor bed and PD-L1 expression on remaining tumor cells, as shown by histological analyses of CEA TCB-treated tumors compared to controls.

Moreover, CEA TCB treatment qualitatively alters the composition of intra-tumor T cells resulting in an increased frequency of activated T cells (expressing CD25) as well as T cells expressing the suppressive marker PD-1 (a hallmark of T cell engagement). Importantly, T cell expansion and activation is not detected in blood (Fig. 5) further confirming that CEA

TCB activity is restricted to CEA-expressing tumor areas. Intravital two-photon imaging of CEA TCB anti-tumor activity further confirmed a high frequency of fragmented (apoptotic) tumor cells along with strong T cell re-localization from tumor periphery into tumor bed already one day after single CEA TCB injection. A detailed analysis of the kinetics of tumor cell killing along with the quantification of intra-tumor T cell number, velocity, crosslinking to tumor cells and the assessment of CEA TCB targeting to tumors is described in Lehmann S et al., (in preparation).

Taken together, the current data show that CEA TCB is a novel tumor-targeted T cell bispecific antibody for treatment of solid tumors with promising anti-tumor activity and the ability to modify the tumor microenvironment. CEA TCB is efficacious in non-inflamed, poorly-infiltrated tumors and converts non-inflamed into highly-inflamed tumors. Phase 1 clinical trials with CEA TCB are currently ongoing. Future studies will focus on combination studies with immune checkpoint modulators to unleash the full potential of CEA TCB-mediated T cell activity against cancer.

## **ACKNOWLEDGEMENTS**

We would like to thank Jackie Sloane Stanley for her help in getting the leukocyte cones;  
Linda Fahrni for kindly supporting the in vitro experiments; Karolin Rommel, Petros  
Papastogiannidis and Nadège Baumlin for conducting in vivo pharmacology studies.

## References

1. Riethmüller. Symmetry breaking: bispecific antibodies, the beginnings, and 50 years on. *Cancer Immun.* 2012.
2. Frankel SR, Baeuerle PA. Targeting T cells to tumor cells using bispecific antibodies. *Curr Opin Chem Biol.* 2013;17:385-92.
3. Baeuerle PA, Reinhardt C. Bispecific T-cell engaging antibodies for cancer therapy. *Cancer Res.* 2009;69:4941-4.
4. Staerz UD, Kanagawa O, Bevan MJ. Hybrid antibodies can target sites for attack by T cells. *Nature.* 1985;314:628-31.
5. Sanford M. Blinatumomab: first global approval. *Drugs.* 2015;75:321-7.
6. Ruf P, Kluge M, Jager M, Burges A, Volovat C, Heiss MM, et al. Pharmacokinetics, immunogenicity and bioactivity of the therapeutic antibody catumaxomab intraperitoneally administered to cancer patients. *Br J Clin Pharmacol.* 2010;69:617-25.
7. Segal DM, Weiner, G.J., Weiner, L.M. Bispecific antibodies in cancer therapy. *Curr Opinion Immunol* 1999.
8. Clinical T. <https://clinicaltrials.gov/>.
9. Hammarström S. The carcinoembryonic antigen CEA family: structures, suggested functions and expression in normal and malignant tissues. *Cancer Biology.* 1999;9.
10. Oikawa S, Inuzuka C, Kuroki M, Matsuoka Y, Kosaki G, Nakazato H. Cell adhesion activity of non-specific cross-reacting antigen (NCA) and carcinoembryonic antigen (CEA) expressed on CHO cell surface: homophilic and heterophilic adhesion. *Biochem Biophys Res Commun.* 1989;164:39-45.
11. Benchimol S, Fuks A, Jothy S, Beauchemin N, Shirota K, Stanners CP. Carcinoembryonic antigen, a human tumor marker, functions as an intercellular adhesion molecule. *Cell.* 1989;57:327-34.
12. Stanners CP, Fuks, A. Properties of adhesion mediated by the human CEA family. In *Cell Adhesion and Communication Mediated by the CEA family: Basic and Clinical Perspectives.* 1998;5:57-71.
13. Chan CHF, Stanners, C.P. Recent advances in the tumour biology of the GPI-anchored carcinoembryonic antigen family members CEACAM5 and CEACAM6. *Current Oncology.* 2007;14.
14. Jessup JaT, P. CEA and metastasis: a facilitator of site-specific metastasis. In *Cell Adhesion and Communication Mediated by the CEA family: Basic and Clinical Perspectives.* 1998;5:195-222.
15. Yoshioka T, Masuko T, Kotanagi H, Aizawa O, Saito Y, Nakazato H, et al. Homotypic adhesion through carcinoembryonic antigen plays a role in hepatic metastasis development. *Jpn J Cancer Res.* 1998;89:177-85.
16. Thomas P, Gangopadhyay A, Steele G, Jr., Andrews C, Nakazato H, Oikawa S, et al. The effect of transfection of the CEA gene on the metastatic behavior of the human colorectal cancer cell line MIP-101. *Cancer Lett.* 1995;92:59-66.
17. Zhou H, Stanners CP, Fuks A. Specificity of anti-carcinoembryonic antigen monoclonal antibodies and their effects on CEA-mediated adhesion. *Cancer Res.* 1993;53:3817-22.
18. Schaefer W, Regula JT, Bahner M, Schanzer J, Croasdale R, Durr H, et al. Immunoglobulin domain crossover as a generic approach for the production of bispecific IgG antibodies. *Proc Natl Acad Sci U S A.* 2011;108:11187-92.
19. Atwell S, Ridgway JB, Wells JA, Carter P. Stable heterodimers from remodeling the domain interface of a homodimer using a phage display library. *J Mol Biol.* 1997;270:26-35.
20. Carter P. Bispecific human IgG by design. *J Immunol Methods.* 2001;248:7-15.
21. Ordonez C, Screaton RA, Ilantzis C, Stanners CP. Human carcinoembryonic antigen functions as a general inhibitor of anoikis. *Cancer Res.* 2000;60:3419-24.
22. Thompson JA, Grunert F, Zimmermann W. Carcinoembryonic antigen gene family: molecular biology and clinical perspectives. *J Clin Lab Anal.* 1991;5:344-66.

23. Conaghan P, Ashraf S, Tytherleigh M, Wilding J, Tchilian E, Bicknell D, et al. Targeted killing of colorectal cancer cell lines by a humanised IgG1 monoclonal antibody that binds to membrane-bound carcinoembryonic antigen. *Br J Cancer*. 2008;98:1217-25.
24. Durbin H. YS, et al. An epitope on carcinoembryonic antigen defined by the clinically relevant antibody PR1A3. *Proc Nati Acad Sci USA*. 1994;91.
25. Klinger M, Brandl C, Zugmaier G, Hijazi Y, Bargou RC, Topp MS, et al. Immunopharmacologic response of patients with B-lineage acute lymphoblastic leukemia to continuous infusion of T cell-engaging CD19/CD3-bispecific BiTE antibody blinatumomab. *Blood*. 2012;119:6226-33.
26. Nagorsen D, Bargou R, Ruttinger D, Kufer P, Baeuerle PA, Zugmaier G. Immunotherapy of lymphoma and leukemia with T-cell engaging BiTE antibody blinatumomab. *Leuk Lymphoma*. 2009;50:886-91.
27. Rathi C, Meibohm B. Clinical pharmacology of bispecific antibody constructs. *J Clin Pharmacol*. 2015;55 Suppl 3:S21-8.
28. Baehner M ea. Antibody fc variants. Patent WO2012130831A1. 2012.
29. Lutterbuese R, Raum T, Kischel R, Lutterbuese P, Schlereth B, Schaller E, et al. Potent Control of Tumor Growth by CEA/CD3-bispecific Single-chain Antibody Constructs That Are Not Competitively Inhibited by Soluble CEA. *Journal of Immunotherapy*. 2009;32:341-52.
30. Oberst MD, Fuhrmann S, Mulgrew K, Amann M, Cheng L, Lutterbuese P, et al. CEA/CD3 bispecific antibody MEDI-565/AMG 211 activation of T cells and subsequent killing of human tumors is independent of mutations commonly found in colorectal adenocarcinomas. *MAbs*. 2014;6:1571-84.
31. Kuroki M, Hachimine K, Huang J, Shibaguchi H, Kinugasa T, Maekawa S, et al. Re-targeting of cytotoxic T lymphocytes and/or natural killer cells to CEA-expressing tumor cells with anti-CEA antibody activity. *Anticancer Res*. 2005;25:3725-32.
32. Holliger P, Manzke O, Span M, Hawkins R, Fleischmann B, Qinghua L, et al. Carcinoembryonic antigen (CEA)-specific T-cell activation in colon carcinoma induced by anti-CD3 x anti-CEA bispecific diabodies and B7 x anti-CEA bispecific fusion proteins. *Cancer Res*. 1999;59:2909-16.
33. Klein C, Sustmann C, Thomas M, Stubenrauch K, Croasdale R, Schanzer J, et al. Progress in overcoming the chain association issue in bispecific heterodimeric IgG antibodies. *MAbs*. 2012;4:653-63.
34. Yan Z, Robinson-Saddler A, Winawer S, Friedman E. Colon carcinoma cells blocked in polarization exhibit increased expression of carcinoembryonic antigen. *Cell Growth Differ*. 1993;4:785-92.
35. Fritsche R, Mach JP. Isolation and characterization of carcinoembryonic antigen (CEA) extracted from normal human colon mucosa. *Immunochemistry*. 1977;14:119-27.
36. Parkhurst MR, Yang JC, Langan RC, Dudley ME, Nathan DA, Feldman SA, et al. T cells targeting carcinoembryonic antigen can mediate regression of metastatic colorectal cancer but induce severe transient colitis. *Mol Ther*. 2011;19:620-6.
37. Du C, Wang Y. The immunoregulatory mechanisms of carcinoma for its survival and development. *J Exp Clin Cancer Res*. 2011;30:12.
38. Kim PS, Ahmed R. Features of responding T cells in cancer and chronic infection. *Curr Opin Immunol*. 2010;22:223-30.
39. Stone JD, Aggen DH, Schietinger A, Schreiber H, Kranz DM. A sensitivity scale for targeting T cells with chimeric antigen receptors (CARs) and bispecific T-cell Engagers (BiTEs). *Oncoimmunology*. 2012;1:863-73.
40. Magee MS, Snook AE. Challenges to chimeric antigen receptor (CAR)-T cell therapy for cancer. *Discov Med*. 2014;18:265-71.
41. Blat D, Zigmund E, Alteber Z, Waks T, Eshhar Z. Suppression of murine colitis and its associated cancer by carcinoembryonic antigen-specific regulatory T cells. *Mol Ther*. 2014;22:1018-28.
42. Griffiths GM, Tsun A, Stinchcombe JC. The immunological synapse: a focal point for endocytosis and exocytosis. *J Cell Biol*. 2010;189:399-406.



43. Stinchcombe JC, Majorovits E, Bossi G, Fuller S, Griffiths GM. Centrosome polarization delivers secretory granules to the immunological synapse. *Nature*. 2006;443:462-5.

## Figure legends

Fig.1. Structure and binding of CEA TCB. (A) Structural characteristics of CEA TCB with Fabs denoting the antibody targeting to CEA (bivalent binding mode), to CD3e (monovalent binding mode), and the Fc with P329G LALA mutation (silent Fc). (B) Median fluorescence intensity (MFI) of binding of CEA TCB to human gastric adenocarcinoma cells (MKN45, EC50 of binding 10 nM) and (C) to human pan T cells, as measured by flow cytometry. The error bars indicate SD based on triplicates.

Fig.2. Assessment of the CEA TCB mode of action. (A) Analysis of CD3 downstream signaling pathway detected at 2, 4 and 6 h of co-culture of Jurkat-NFAT-luc cells, MKN45 tumor cells and increasing concentrations of CEA TCB. RLU, relative luminescence units corresponding to the intensity of luciferase expression downstream of CD3. (B) Merged immunofluorescence images of MTOC localization phenotypes seen in cytotoxic T cell lymphocyte (CTL) conjugates with tumor cells: MTOC is docked at the synapse (i.e. in contact with the membrane marker), MTOC is proximal to synapse, and MTOC is distal to synapse (i.e.  $\geq 50\%$  distance of total cell length). Cells are labeled with antibodies against talin (green), CD8 (white), and  $\gamma$ -tubulin (red), scale bar represents 5  $\mu$ m. White arrows indicate T-cells. Graph displays the quantification of MTOC re-localization in CTL after treatment with CEA TCB (n = 490), Untargeted TCB (n= 377), and no therapy (n= 416). Error bars show standard deviation from the means of three independent experiments. A Dunnett two-way anova test for increase in MTOC docking in CEA TCB samples compared to the untargeted TCB and no therapy control showed statistical significance ( $p < 0.0001$ , adjusted for multiple hypothesis testing). (C) Merged immunofluorescence images of perforin

polarization to the immunological synapse seen in CTL conjugates with tumor cells: perforin is clustered/polarized at the synapse, perforin is dispersed around the cell or is distal from synapse (i.e. >80% of distal perforin). Cells are labeled with antibodies against talin (green) and perforin (red). White arrows indicate T-cells (distinguished by CD8 staining, not shown), scale bar represents 5  $\mu$ m. Graph displays the quantification of perforin polarization in CTLs after treatment with CEA TCB (n= 294), untargeted TCB (n= 354), and no therapy (n= 404). Error bars show standard deviation from the means of three independent experiments. A Dunnett two-way anova test for increase in perforin polarization in CEA TCB samples compared to the untargeted TCB and no therapy control showed statistical significance ( $p < 0.0001$ , adjusted for multiple hypothesis testing). (D-E) Kinetic analysis of early T cell activation (CD69 expression on CD8 and CD4 T cell subsets) detected at 8.5, 25 and 48 h post incubation of LS174T colon carcinoma cells with CEA TCB and human PBMCs (E:T 10:1). (F) Dose and time-dependent tumor cell lysis detected at 8.5, 25 and 48 h post incubation with CEA TCB, human PBMCs and LS174T cells (E:T 10:1). (G) Quantification of cytokines and cytotoxic granules released into culture supernatants as result of T cell activation upon CEA TCB-mediated tumor cell killing (targets MKN45 cells, effectors human PBMCs, E:T 10:1, detection after 48 h). Error bars represent SD of triplicates. Calculated EC50 values: IFN $\gamma$  1.4 nM, TNF $\alpha$  809 pM, IL-2 = 473 pM, IL-6 = 338 pM, and IL-10 = 432 pM, granzyme B = 445 pM. (H) Assessment of CD8 and CD4 T cell proliferation and (I) late T cell activation (CD25 expression) detected 5 days after CEA TCB-mediated lysis of MKN45 cells in presence of human PBMCs (E:T 10:1). T cell proliferation was detected by CFSE dye dilution (methods) with proliferation peaks illustrated in panel I.

Fig. 3. Correlation between CEA expression and CEA TCB activity. (A) Analysis of tumor cell lysis 48 h post incubation with CEA TCB and human PBMCs (E:T 10:1). Tumor target

cells, expressing varying levels of CEA were MKN-45, LS174T and HT29. The primary colon epithelial cell line shown in the graph is CCD-841). Details of the cell lines are listed in Table S1. (B) Percentage of tumor cell lysis mediated by 20 nM CEA TCB with rank plots displaying the correlation between CEA expression level (CEA binding sites) and tumor lysis for the non-responders (in red) and the responders (in blue) groups. CEA binding sites equal to surface receptor expression measured by flow cytometry using Qifikit (Table S1). (C) The responders have significantly higher expression of CEA binding sites than the non-responders (Mann-Whitney test,  $P < 0.0001$ ).

Fig. 4. In vivo efficacy and intravital two-photon imaging of CEA TCB activity in tumor/PBMC co-grafting model. Isolated human PBMC were mixed with the human colon carcinoma cell line LS174T stably transfected with plasmid coding for firefly luciferase (LS174T-fluc2) at E:T (PBMC:tumor cells) ratio of 5:1 (A, B), 1:1 (C, D) and injected s.c. in NOG mice. CEA TCB was administered twice/week i.v. at 2.5 mg/kg, starting either one day or seven days after PBMC/tumor cell co-grafting, as indicated. Control groups received phosphate-buffer saline (PBS, vehicle) or an untargeted TCB at a dose of 2.5 mg/kg starting one day after co-grafting. Tumor volume was measured by digital caliper, (A and C), and tumor growth by bioluminescence (total flux), (B and D). (A) Tumor growth of individual mice ( $n = 12$ ) at E:T 5:1 and (C) E:T 1:1. (B) Average tumor burden and standard error of mean (SEM,  $n = 12$ ) measured by bioluminescence (total flux) for E:T 5:1 and (D) 1:1.

Statistical analysis, one way analysis of variance (ANOVA) followed by Tukey test.

Significant differences are reported for each group at study termination (day 19 or day 23 for B and D, respectively) as compared to vehicle group (\*\* $p < 0.01$ ), ns=not significant. (E)

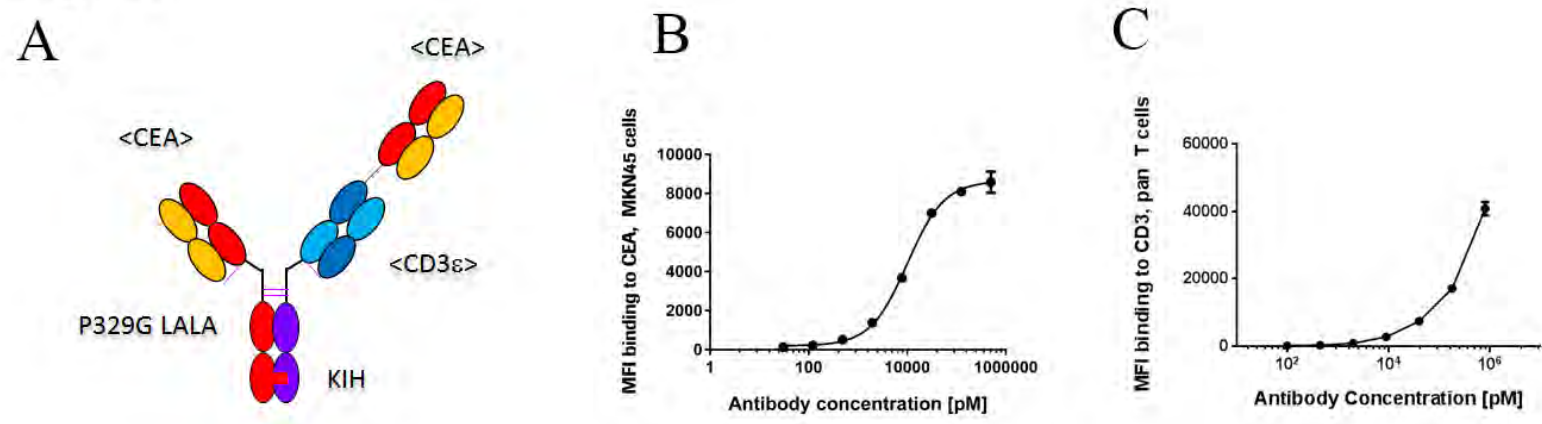
Two-photon microscopic images of tumor cells/T-cell co-grafts implanted into the dorsal skinfold chamber at baseline (4 days after PBMC/tumor co-grafting), and 1 day or 6 days after CEA TCB or untargeted TCB treatment. The same animals were imaged at baseline and

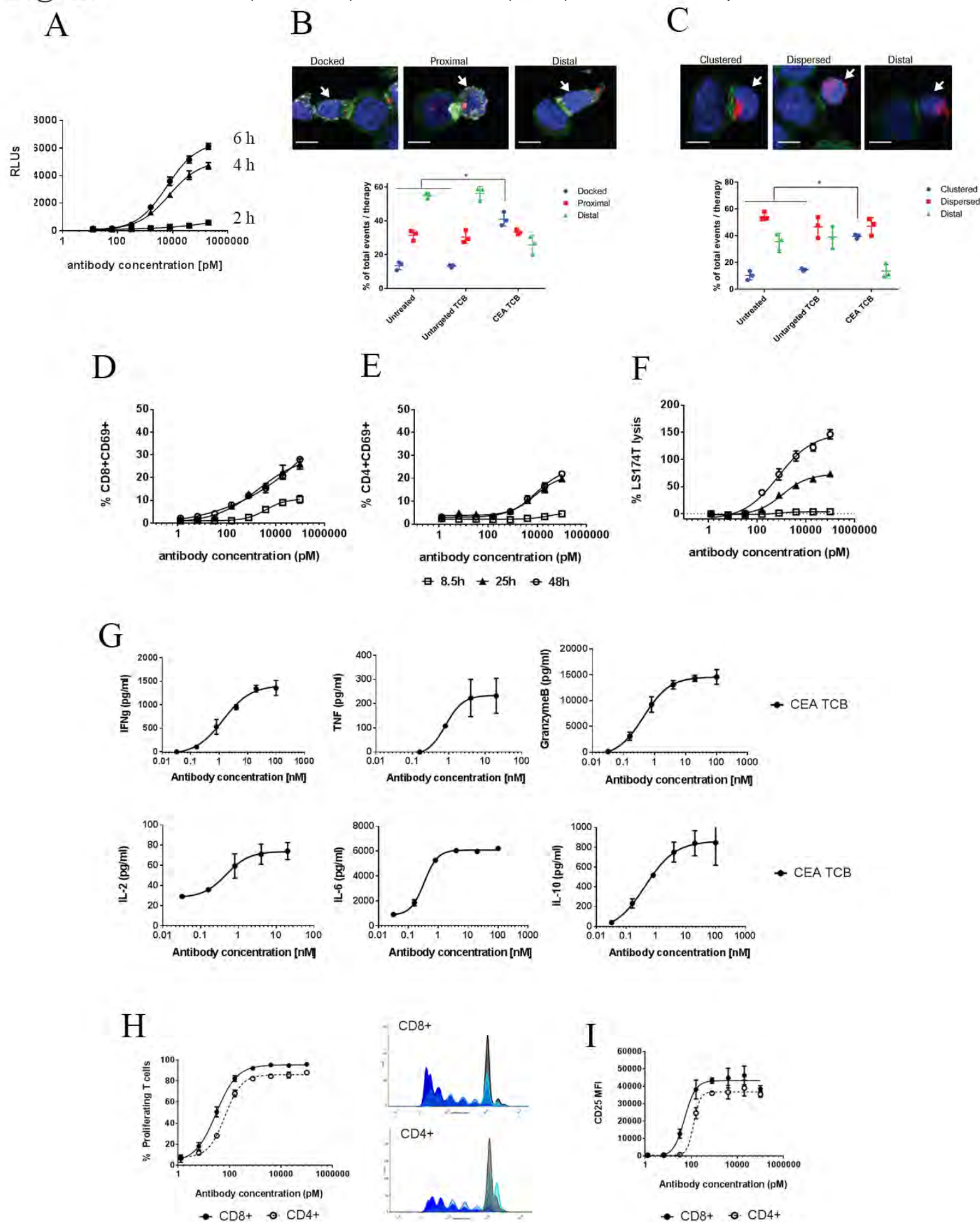
one day post TCB treatment (left and middle panels). Tumor cells, red; T cells, green. Bars, 50  $\mu$ m. Right panels show two-photon microscopic images acquired on separate animals 7 days after TCB antibody treatment. Tumor cells, red; Second harmonics (SHG) signal, gray. Bars, 50  $\mu$ m.

Fig. 5. In vivo activity of CEA TCB in xenograft model with i.p. transfer of human PBMCs. (A) LS174T-fluc2 cells were injected s.c. into NOG mice and left to grow for 7 days. Human PBMCs were transferred by i.p. injection ( $10 \times 10^6$  cells, red arrow). Mice were treated with CEA TCB or untargeted TCB at 2.5 mg/kg, twice/ week, i.v., starting at day 10 after tumor cell injection (3 days post PBMC transfer) (blue arrow). Control groups received either phosphate-buffer saline (PBS, vehicle) or untargeted TCB. Tumor growth was measured by caliper twice/week. Graphs display the tumor growth curves of individual mice (n =8-10). (B) Tumor volume at day 20 after tumor cell injection. Statistical analysis: one way analysis of variance (ANOVA) followed by Tukey test, \* $p < 0.05$ . (C) Flow cytometry analysis of human T cells in blood and explanted tumors at study termination. Single cell suspensions were stained with anti-huCD45 and anti-huCD3 antibodies. Percentages of human T cells are shown for representative mice out of 3-7 analyzed/group. Bar graphs report the percentage of human T cells (huCD3) in blood and tumor in the different groups, for all mice analyzed at study termination. (D) Flow cytometry analysis of T cell activation by assessing huCD25 and huPD-1 expression in blood and in tumor. Histogram plots from representative mice (out of 3-7 analyzed/group) are shown (E) Representative images of histological analysis of explanted tumors stained for human CEA, human CD45, human CD4 and human CD8 (all brown). Areas from the CEA panels (enumerated squares 1) were selected to display CD45, CD4 and CD8 immune cell localization in the tumor bed (enumerated squares 2) and in the tumor periphery (enumerated squares 3). Scale bare is indicated on each panel. (F) Representative images of histological analysis of explanted tumors stained for H&E and

human PD-L1. Areas from the H&E panels (enumerated squares 1) were selected to display PD-L1 expression (brown staining); selected areas from the PD-L1 panels (enumerated squares 2) were further enlarged to show a detailed view of PD-L1 expression. Representative images of at least 3 mice analyzed/group. Samples were counterstained with hematoxylin (blue).

**Fig. 1.**







**Fig. 3.**

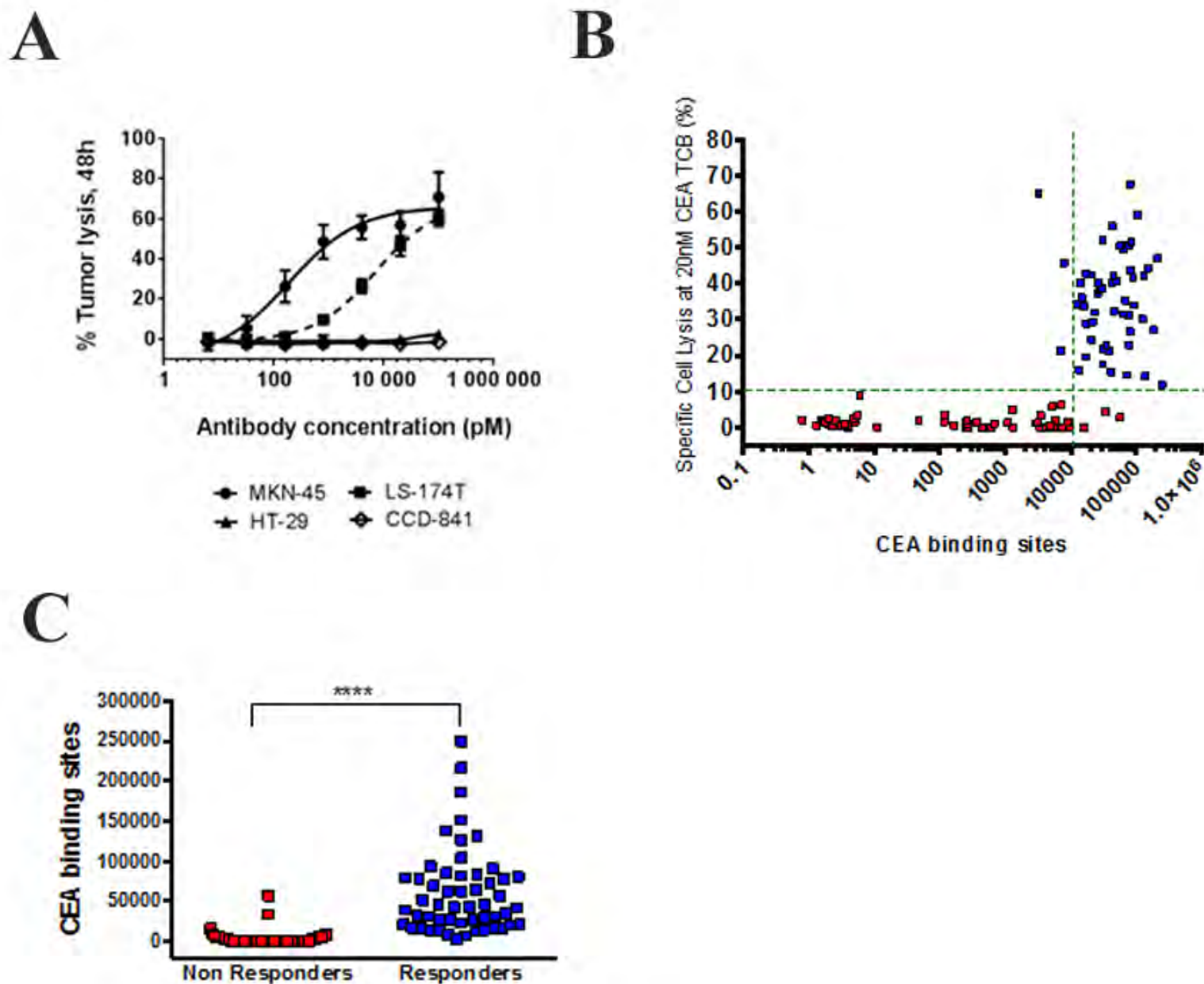




**Fig. 4.**

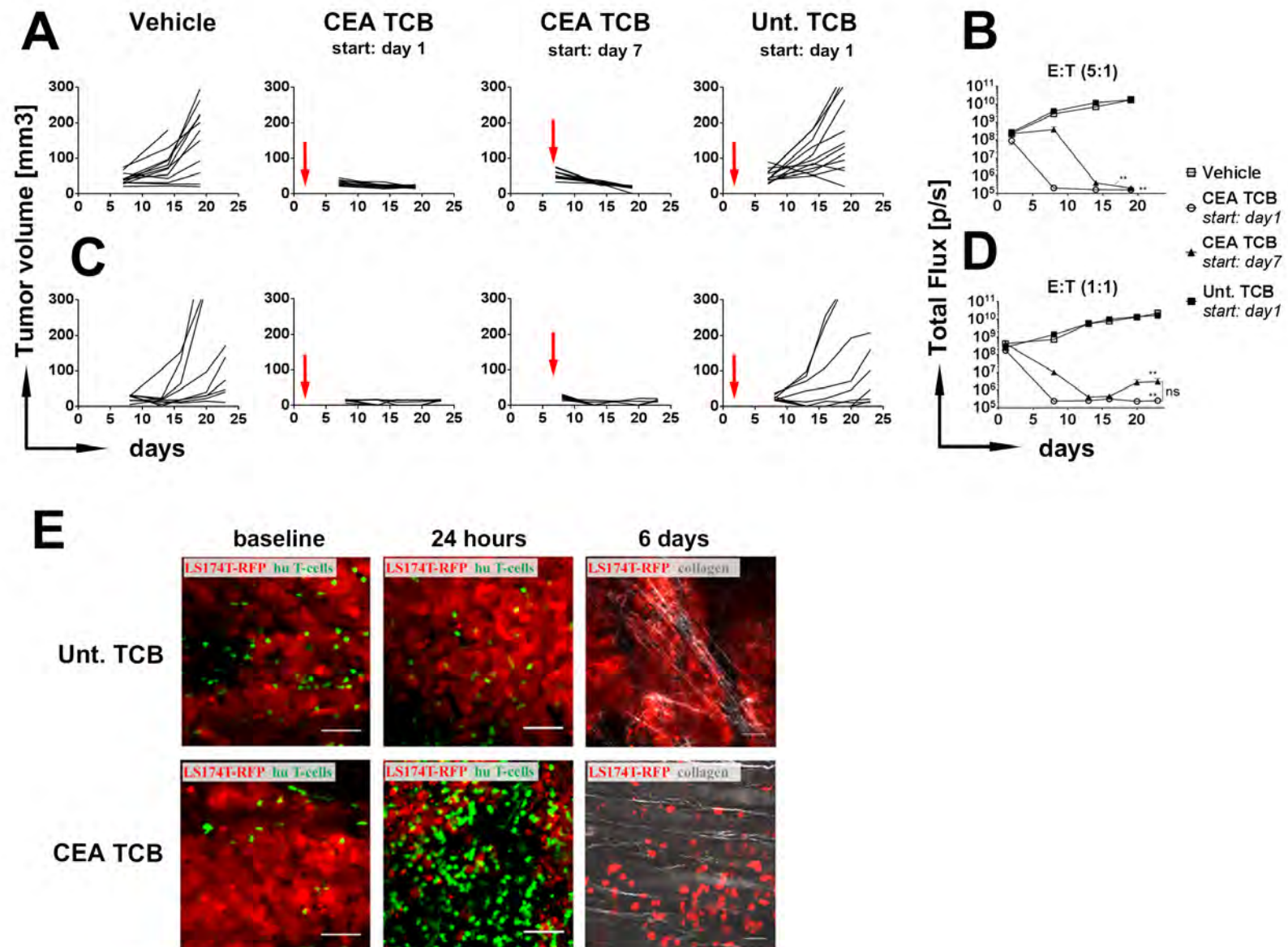
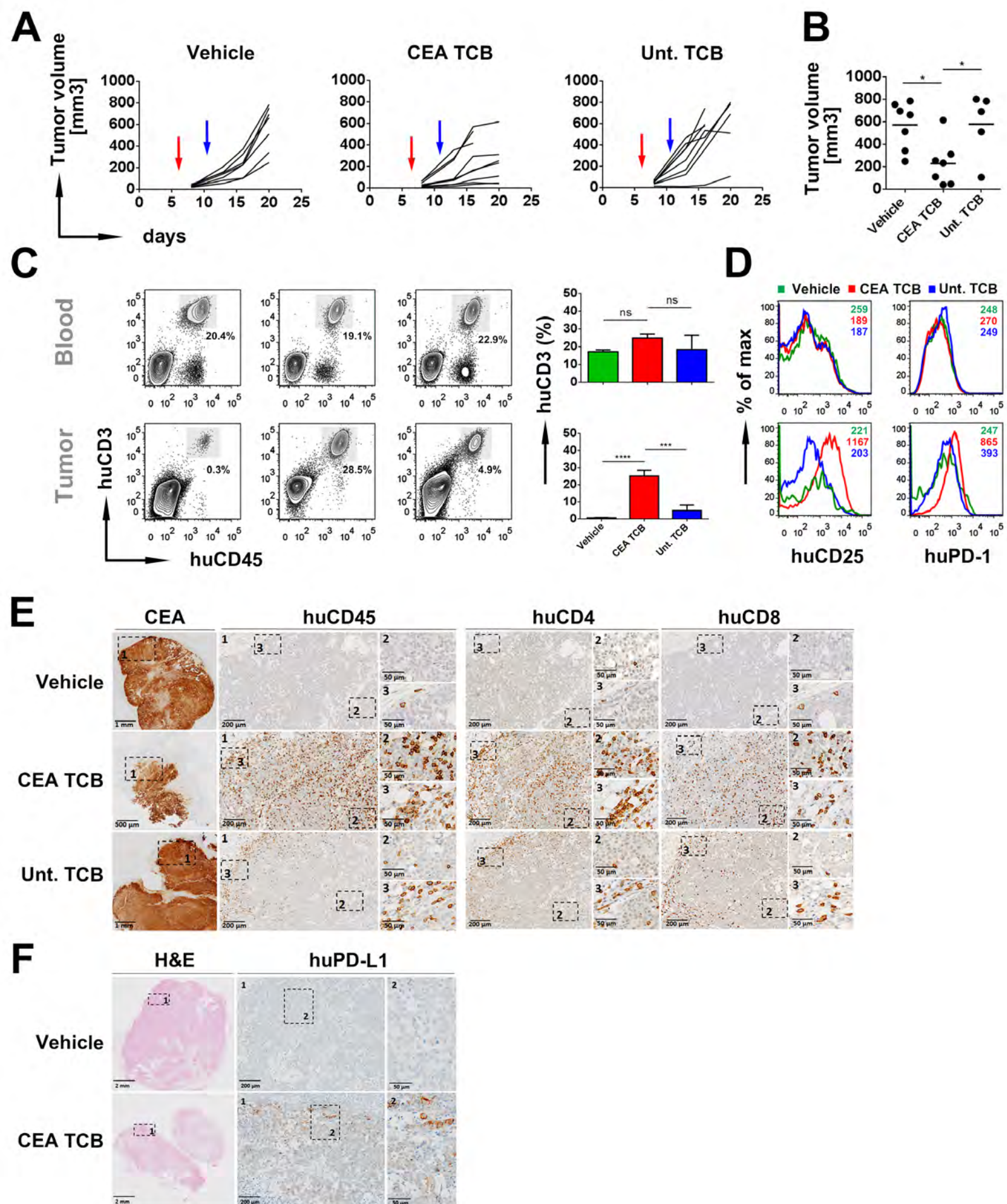


**Fig. 5.**



# Clinical Cancer Research

## A NOVEL CARCINOEMBRYONIC ANTIGEN T CELL BISPECIFIC ANTIBODY (CEA TCB) FOR THE TREATMENT OF SOLID TUMORS

Marina Bacac, Tanja Fauti, Johannes Sam, et al.

*Clin Cancer Res* Published OnlineFirst February 9, 2016.

<b>Updated version</b>	Access the most recent version of this article at: doi: <a href="https://doi.org/10.1158/1078-0432.CCR-15-1696">10.1158/1078-0432.CCR-15-1696</a>
<b>Supplementary Material</b>	Access the most recent supplemental material at: <a href="http://clincancerres.aacrjournals.org/content/suppl/2016/02/06/1078-0432.CCR-15-1696.DC1.html">http://clincancerres.aacrjournals.org/content/suppl/2016/02/06/1078-0432.CCR-15-1696.DC1.html</a>
<b>Author Manuscript</b>	Author manuscripts have been peer reviewed and accepted for publication but have not yet been edited.

<b>E-mail alerts</b>	<a href="#">Sign up to receive free email-alerts</a> related to this article or journal.
<b>Reprints and Subscriptions</b>	To order reprints of this article or to subscribe to the journal, contact the AACR Publications Department at <a href="mailto:pubs@aacr.org">pubs@aacr.org</a> .
<b>Permissions</b>	To request permission to re-use all or part of this article, contact the AACR Publications Department at <a href="mailto:permissions@aacr.org">permissions@aacr.org</a> .